



Buoyancy-Driven Ventilation in the Interior-Most Flats of an Apartment Building with Different Corridor Vent Opening Condition

Soma Kalia¹, Nibedita Mishra², Prakash Ghose^{3,*}

¹ Department of Home Science, Ramadevi Women's University, Bhubaneswar- 751007, India

² Department of Home Science, Puri Woman's college, Ramadevi Women's University, Bhubaneswar- 751007, India

³ School of Mechanical Engineering, KIIT Deemed to be University, Bhubaneswar-751024, India

ARTICLE INFO

ABSTRACT

Article history:

Received 11 April 2023

Received in revised form 24 August 2023

Accepted 17 October 2023

Available online 30 December 2023

Keywords:

Buoyancy-driven ventilation; Apartment;
Corridor vent; CFD

In the present work, computational simulations are conducted for an apartment building to investigate the buoyancy-driven airflow in the corridor and inside the rooms. Two types of corridor vent openings are provided through which the hot light air moves to the ambient. Two floors are considered for the study. The simulations are conducted with three different temperature difference conditions between walls and room inside air such as; $\Delta T=10^{\circ}\text{C}$, $\Delta T=15^{\circ}\text{C}$, $\Delta T=20^{\circ}\text{C}$ for two different corridor vent opening configurations. When the corridor vent openings are kept only in front of the doors and windows, recirculation zones below the roof near the air entry region are observed and part of the air escaped through the inlet. In the case of a wide corridor vent opening, air does not escape through the inlet. With increase in ΔT , the airflow increases irrespective of vent positions. Mainly the area of the rooms is well ventilated closer to the door position. It is also observed that the lower floor is relatively well-ventilated as compared to the upper floor. The ACH increases with increase in vent opening and it also increases with increase in ΔT .

1. Introduction

The movement of atmospheric airflow inside the house by natural means is designated as natural ventilation. Air flow around the human body enhances the convective heat transfer and evaporation rate, thus the desired body temperature is maintained, which is essential to keep the human healthy mentally and physically as mentioned by Li *et al.*, [1]. Effective natural ventilation also can full fill the requirement of the NetZero energy housing concept. Developing countries are moving forward with emerging economic growth due to rapid industrialization. As a result, immigration from rural areas to urban areas causes an increase in population in prominent cities [2]. However, in order to accommodate these huge immigrants, multi-stories apartments are built in large numbers in big cities across the country.

* Corresponding author.

E-mail address: pghosefme@kiit.ac.in

<https://doi.org/10.37934/araset.36.2.3655>

Keeping in view of purchasing capacity of the majority of the population, many cheap high-rise apartments are being constructed, where the open spaces for ventilation are compromised. It has been observed that narrow spaces are kept in between blocks and so many common walls are there in between the houses, which adversely affects the natural ventilation. However, mechanical ventilation may be an alternative but a huge energy crisis and energy price is a major challenge for the middle class in developing countries [3]. Therefore, more focus should be given to natural ventilation in apartment buildings that are situated particularly in overcrowded developing countries.

Buoyancy-driven ventilation or stack ventilation is one of the natural phenomena through which air circulation occurs inside the house. The temperature difference between the wall and room air drives the air out of the building. Due to solar radiation, the wall and top roof of buildings become hot and the room air temperature is relatively cooler than the wall. Therefore, due to the temperature difference, the heat transfers from the hot wall to the room air. As a result, the room air becomes lighter and moves in the upward direction and the provision of the vent on the roof and building corridor, allows the hot air to move out to the ambient. Consequently, the fresh air moves into the building through various openings. Ghazali *et al.*, [4] performed a case study on the indoor thermal comfort of a naturally ventilated atrium zone in public market. The temperature, relative humidity and airflow velocity are measured throughout the day and it is found that the parameters are not as per the suggested comfort value. Hence, few suggestions are given to improve the ventilation, so that comfort ambience can be obtained.

Walker *et al.*, [5] conducted experimentation to investigate the buoyancy-driven ventilation effect of a scaled model building and by applying the similarity analysis CFD simulation are conducted for real-size buildings. It has been reported that with stack opening condition, the room temperature decreases as compared to stack closed condition. Moreover, the room temperature difference between stack opening and closed conditions rises for higher floors. Liu *et al.*, [6] investigated stack ventilation in an atrium building using CFD. It is reported that only buoyancy-driven ventilation is not sufficient for hot and humid climates for low-rise buildings. Some additional ventilations such as wind-driven ventilation and mechanical driven are required. Andrew and Gary [7] developed a mathematical model for stack ventilation in a multi-compartment building. They observed that in order to minimize the disparity of airflow rate between stories of the building, the control of ventilation flows must be shared among all ventilation openings in the building. Yang and Li [8] proposed a hybrid approach for ventilation. It has been mentioned that to obtain proper ventilation through buoyancy driven flow, the stack should be sufficiently high. In order to avoid a tall stack, it has been proposed that upper floors should be provided with a mechanical ventilation system, whereas the lower floors should be naturally ventilated. Tovar and Garrido [9] simulated the transient airflow behaviour of two interconnected rooms, sharing a single opening. The exterior vent opening is provided at the floor level of a room whereas, near the roof of the other room, cold air is stacked. Hence, a negative buoyancy airflow is investigated that mimics the split air condition position. It has been observed that by lowering the intermediate opening, the cold fluid density increases at a higher rate. Jing *et al.*, [10] performed a CFD simulation, following the experimentation to improve buoyancy-driven flow in and around the hot corridor of a factory building. From the study, it has been observed that the height of the heat source significantly affects the thermal environment. Kotani *et al.*, [11] designed the bottom portion of the light well (void). With the help of a simple calculation, the void temperature distribution along the vertical direction and the ventilation rates are predicted. Shaun and Andrew [12] investigated the influence of the ratio of window position height and stack height (h_B/h_A) on the flow pattern inside the house for a buoyancy-driven airflow. It has been reported that when $h_B < h_A$, inflow occurs through vent *B* and outflow occurs through the

stack vent A and vice versa. Schulze and Ursula [13] investigated a steady-state buoyancy-driven airflow with different temperature and pressure difference conditions at various openings of the house with various opening types. It has been concluded that control over the opening plays an important role in proper ventilation. Bayoumi [14] studied the airflow improvement in the classroom through an interconnected naturally ventilated corridor. It has been reported that the airflow can be improved by 14.5 times with the provision of a both-side opening interconnected corridor as compared to a single-sided classroom ventilation system. CFD (computational fluid dynamics) is a virtual tool that has been widely used to investigate the fluid flow behaviour with a greater accuracy level [15-18]. Bayoumi [19] investigated the ventilating effect through a hybrid ventilation system (Mechanical and buoyancy-driven flow) in a hot climate like Saudi Arabia. In their CFD work, they presented a novel method for energy saving in university buildings. Hussain and Patrick [20] investigated the thermal condition of the atrium space of a commercial building considering solar assisted buoyancy driven ventilation through CFD simulation. They also tested the prediction ability of various turbulent models. Effect of radiation has also been considered in their work. The simulations were conducted with window blind open and closed conditions. It is observed that with window blind open condition, the air flow becomes better. Acred and Hunt [21] studied the buoyancy driven flow regime of an multi-story atrium building. It is reported that if the atrium vent area will be too small a reverse flow will occur at the top floor. On the other hand, with a larger atrium vent, a recirculation can be observed near the vent. Hence, in order to get proper ventilation in all the floors, atrium vent opening should be optimized.

With a literature review process, it has been noticed that mainly, the buoyancy-driven natural ventilation process is conducted for a single hall in the multi-story building using an atrium. The effect of atrium height and wall vent positions are also investigated by a few researchers. Few kinds of research are conducted for two side opening room interconnected corridors for improved airflow. A corridor pathway opening vent may be a better option, which allows the hot air to move in the upward direction. Hence, room hot air may also be sucked along with light air, causing room ventilation. However, physically steel grills should be placed on the pathway corridor holes so that one can walk on them.

In this paper, a CFD study has been performed on buoyancy-driven natural ventilation of an apartment situated in the tropical climatic city, of Bhubaneswar, India. Since its climate is hot and humid, major time of the year, particularly in summer, ventilation is very much necessary. An existing apartment plan is considered for the study, which is situated on the northern side of the city. Only two floors are considered for the study. The corridor openings just in front of the doors and windows and the corridor opening in the remaining area of the corridor are mainly focused in this study. The temperature difference between the walls, roof and the air inside the rooms are varied to investigate the airflow. The CFD simulation has been carried out with the help of the commercial CFD tool Ansys Fluent 19.2.

2. The Motivation for the Study

Bhubaneswar city, India is located at 20.2961° N, 85.8245° E from the standard global position. The city is located in a hot tropical climatic region. The month-wise last ten years (2010-2020) of weather data of Bhubaneswar city, such as; maximum dry bulb temperature and maximum relative humidity are collected from www.weatheronline.com [22]. The maximum values are used for analysis because; the design should always be made for the worst conditions. The maximum values of DBT and relative humidity are used in the Psychometric chart to find out the months that fall under the comfort zone as shown in Figure 1. The comfort zone is taken in between 22°C-27°C DBT and

40%-60% relative humidity referring from [23]. However, it has been observed that the months in the winter season are somehow closer to the comfort zone. Particularly, in the summer season the weather condition is much beyond the comfort zone. Therefore, year-round ventilation is necessary for this desired location and this is the motivation factor of the current research.

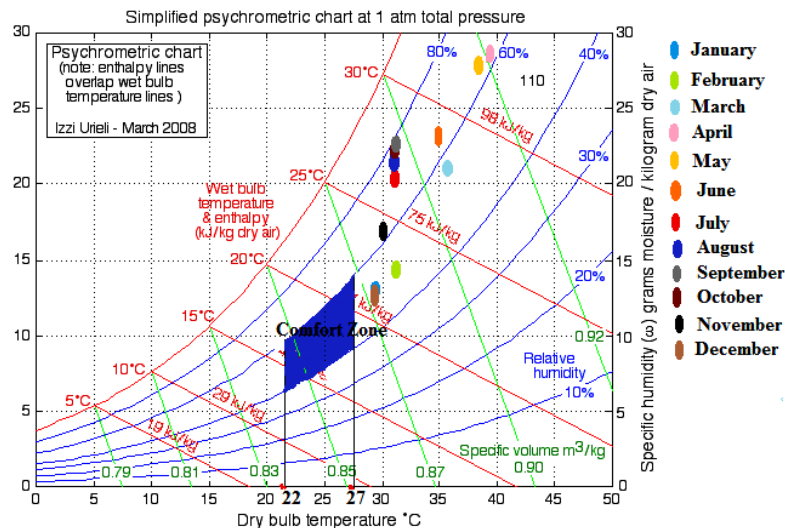


Fig. 1. Psychrometric chart that presents the weather condition of different months

3. Physical Model

Three-dimensional models are prepared considering the actual dimensions of block 'B' of an existing apartment, which is located on the northern side of Bhubaneswar city. Figure 2(a) illustrates block 'B' where floor numbers and flat numbers of the fifth floor are given. On each floor, flat sizes are the same. The parking ground floor is not considered in this study. Moreover, the ventilation inside the kitchen and bathrooms is also excluded from this study considering less percentage of time spent by occupants in these rooms. In this work, the innermost flats are considered for the study, because these flats are blocked by neighbouring flats from one side and also very less space is there in between blocks on the other side. As a result, poor ventilation is expected in these flats. From Figure 2(b), one can envisage that, flat no. 302, 303, 306 and 307 on the third floor are the innermost flats in the block. In order to see the ventilating effect for worst conditions in these innermost flats, it is assumed that all the doors and windows of all neighbouring flats on the same floor and all the flats on other floors are closed. All the flats of the neighbouring blocks are also assumed as closed. So passive ventilation will be excluded in this way. Only the bouncy-driven ventilation is considered. Moreover, these assumptions lessen the computational cost as well.

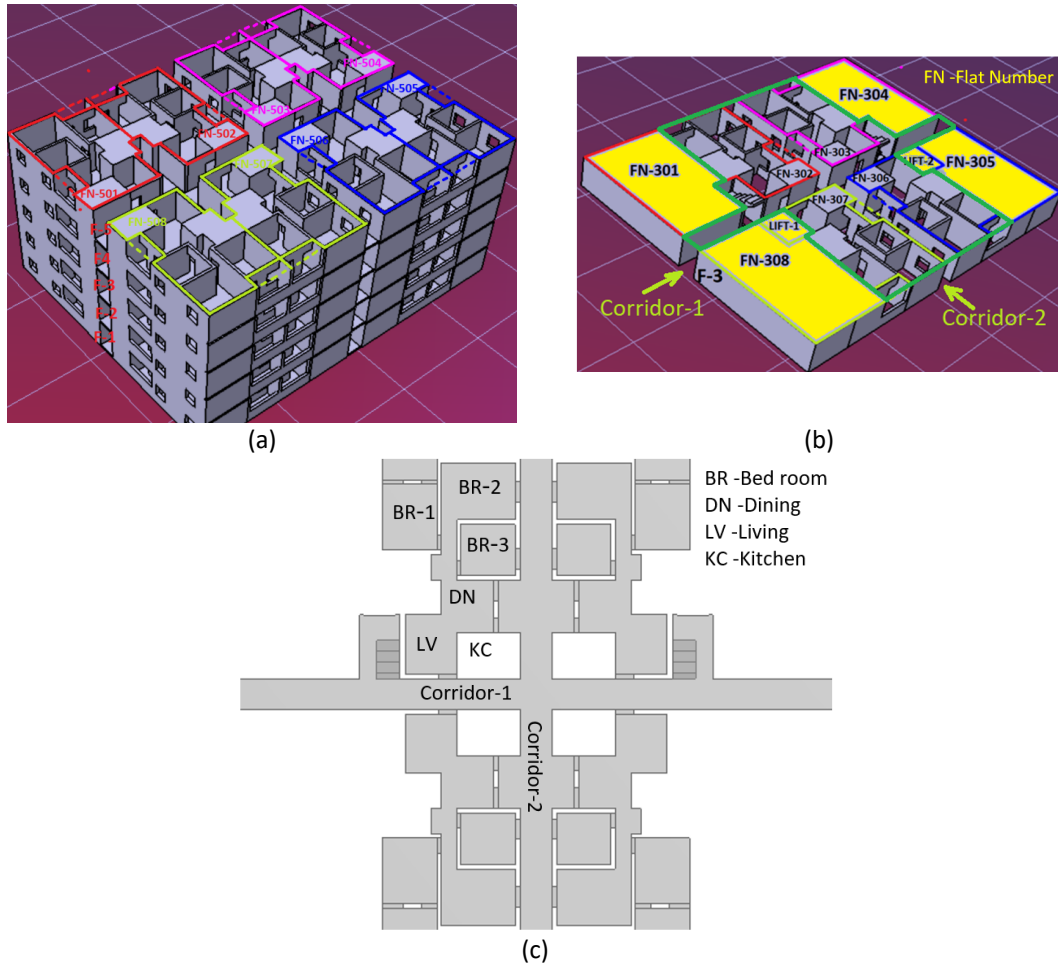


Fig. 2. (a) A three-dimensional model of block B of an existing apartment located in Bhubaneswar, India (b) Domain of interest for computation (c) Floor plan

4. Computational Modelling

This is a buoyancy-driven airflow problem. Therefore, conservation of mass and momentum and energy equations are solved to obtain pressure and velocity distribution. Since the problem is turbulent in nature, time-averaged mass conservation and RANS equations are solved. In order to evaluate the Reynolds stresses, the Boussinesq equation is used. For the evaluation of eddy viscosity required to solve Boussinesq, the standard k-ε turbulent model is used. The governing equations are given as follows;

i. Conservation of mass

$$\frac{\partial}{\partial x_i} (\rho \bar{u}_i) = 0 \quad (1)$$

ii. Conservation of momentum

$$\frac{\partial}{\partial x_i} (\rho \bar{u}_i \bar{u}_j) = -\frac{\partial \bar{p}}{\partial x_i} + \frac{\partial}{\partial x_j} (\bar{\tau}_{ij} - \rho \overline{u'_i u'_j}) + S_m \quad (2)$$

iii. Conservation of energy

$$\frac{\partial}{\partial x_i} (\rho \bar{u}_j \bar{h}) = \frac{\partial}{\partial x_i} \left(\frac{\mu}{\sigma} \frac{\partial \bar{h}}{\partial x_i} - \rho \overline{h'' u_j''} \right) \quad (3)$$

where, ρ is the density of the fluid and \bar{u}_i and \bar{p} are the time average mean flow velocity and time average mean pressure. The stress tensor in the momentum equation is expressed as.

$$\bar{\tau}_{ij} = \mu \left(\frac{\partial \bar{u}_i}{\partial x_j} + \frac{\partial \bar{u}_j}{\partial x_i} \right) \quad (4)$$

$-\rho \overline{u_i' u_j'}$ is the Reynolds stress and $\rho \overline{h'' u_j''} = \frac{\mu_t}{\sigma_t} \frac{\partial \tilde{h}}{\partial x_i}$ is the turbulent flux in the energy equation. These additional terms are formed through time averaging of instantaneous governing equations. $S_m = \rho g \beta (T - T_\infty)$ (Boussinesq approximation) is the source term in Y-momentum equation. This term controls the air movement due to the temperature difference of air inside the computational domain, where the term β is the thermal expansion coefficient. β is evaluated as the inverse of the sum of wall and room air temperature in Kelvin.

Two transport equations are solved to obtain the rate of generation of turbulent kinetic energy (k) and dissipation rate of turbulent kinetic energy (ϵ), respectively. The assumption for this model is that the flow is fully turbulent (high Reynolds number). In the standard k - ϵ model [24], the governing equations for k and ϵ are expressed as follows:

$$\frac{\partial}{\partial x_i} (\rho k \bar{u}_i) = \frac{\partial}{\partial x_j} \left[\left(\mu + \frac{\mu_t}{\sigma_k} \right) \frac{\partial k}{\partial x_j} \right] + G_k + \rho \epsilon \quad (5)$$

$$\frac{\partial}{\partial x_i} (\rho \epsilon \bar{u}_i) = \frac{\partial}{\partial x_j} \left[\left(\mu + \frac{\mu_t}{\sigma_\epsilon} \right) \frac{\partial \epsilon}{\partial x_j} \right] + C_{1\epsilon} \frac{\epsilon}{k} G_k - C_{2\epsilon} \rho \frac{\epsilon^2}{k} \quad (6)$$

In the above equations, G_k represents the generation of turbulent kinetic energy, which is expressed in terms of the mean velocity values as,

$$G_k = \left(\mu_t \left(\frac{\partial \bar{u}_i}{\partial x_j} + \frac{\partial \bar{u}_j}{\partial x_i} \right) - \frac{2}{3} \rho k \delta_{ij} \right) \frac{\partial \bar{u}_j}{\partial x_i} \quad (7)$$

Turbulent viscosity can be obtained from the dimensional analysis as given below

$$\mu_t = C_\mu \rho v l = C_\mu \rho \frac{k^2}{\epsilon}, \text{ where } C_\mu \text{ a model constant and its value is taken as 0.09.}$$

$$v = k^{1/2}, l = \frac{k^{3/2}}{\epsilon}, \text{ where } v \text{ is the velocity scale and } l \text{ is the length scale}$$

The model constants $C_{1\epsilon}$, $C_{2\epsilon}$, σ_k (turbulent Prandtl number for k) and σ_ϵ (turbulent Prandtl number for ϵ) in the k and ϵ equations have default values obtained empirically.

4.1 Boundary Condition and Meshing

In this study, only two floors of the most interior block have been considered. Two different corridor openings have been considered for the buoyancy-driven airflow. Figure 3(a) shows the boundaries of the computational domain with the provision of corridor-opening vents in front of the doors and windows and Figure 3(b) shows the computational domain with the provision of corridor-

opening vents, except the areas in front of the doors and windows. The vent openings are given on both floors of the building. Pressure inlet and pressure outlet boundaries are shown in Figures 3(a) and 3(b). The remaining parts are taken as wall boundaries. The temperature of the wall is taken equal to the ambient temperature in summer. The temperature of the air inside the house is kept less than the ambient temperature. The heat transfer from the wall to the air inside the house increases the air temperature near the wall. As a result, due to the temperature difference of air near the wall and the remaining areas, air movements occur.

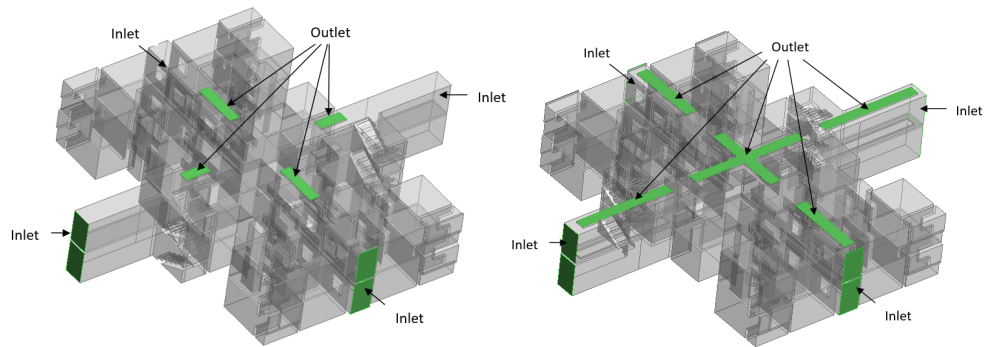


Fig. 3. Computational domain and the boundaries (a) corridor opening vents in front of the doors and windows (b) corridor opening vents area except for the areas in front of the doors and windows

Two computational geometries are prepared for two different corridor vent positions. The geometries are discretized with four different numbers of elements. Figure 4 shows the meshed geometry of the flat with corridor vent provision in front of the doors and windows. It is discretized with 2.6 million elements. A sectional view is also given in this figure. Unstructured tetrahedron elements are used for the meshing. In order to verify the independency of the grid on the results, the grid independence test is also conducted. The geometry of the flat with corridor vent provision in front of the doors and windows is discretized with 1.5, 1.8, 2.3 and 2.6 million elements and simulations are conducted with $\Delta T=15^{\circ}\text{C}$ condition. The average velocities at the four corridor entries are compared.

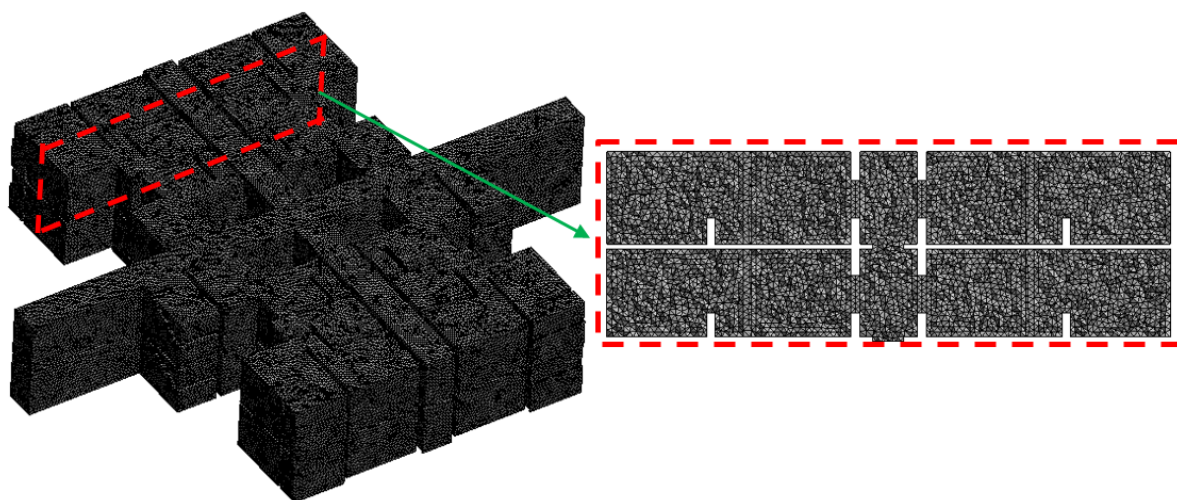


Fig. 4. Meshing with 2.6 million cells

Table 1 shows the grid independence test. A negligible variation in result in between 2.3 and 2.6 million of element domain is observed. However, 2.3 million cell geometry is used for further

simulations. Similarly, the grid independence study for the geometry is also conducted where a corridor opening vent is provided in the remaining area except the area in front of the doors and windows.

The various governing equations, k-ε turbulent model are used in this computational work are used and validated by various researchers [25-27] for the investigation of buoyancy-driven ventilation in commercial and residential buildings. Hence, the computational models used in this work are already well-validated.

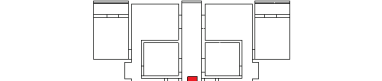
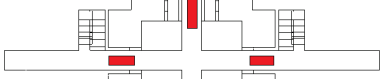
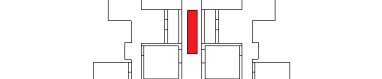
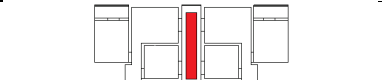

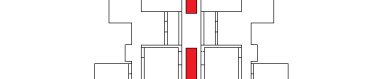
Table 1
 Grid independence test

Variables	1.5 million cell mesh domains	1.8 million cell mesh domains	2.3 million cell mesh domains	2.6 million cell mesh domains
The mass-weighted average velocity of corridor inlets of corridor-1 in m/s for Case-A-2	0.6023	0.6255	0.6469	0.6502
The mass-weighted average velocity of corridor inlets of corridor-2 in m/s for Case-A-2	0.5832	0.6298	0.6521	0.6588

5. Results and Discussion

Six different cases are simulated as shown in Table 2 Case-A-1 to A-3 are the cases for corridor opening in front of doors/ windows when the temperature difference between the wall and inside air is 10°C, 15°C and 20°C respectively. Similarly, case-B-1 to B-3 are the cases for the corridor opening remaining part except in front of doors/windows when the temperature difference between the wall and inside air is 10°C, 15°C and 20°C respectively.

Table 2
 Various cases

Case	Corridor opening position	Wall temperature (K)	Temperature difference ΔT (K)
Case A-1	Corridor opening in front of doors/ windows		10
Case A-2	Corridor opening in front of doors/ windows		15
Case A-3	Corridor opening in front of doors/ windows		20
Case B-1	Corridor opening remaining part except in front of doors/windows		10
Case B-2	Corridor opening remaining part except in front of doors/windows		15
Case B-3	Corridor opening remaining part except in front of doors/windows		20

In Figure 5, a clear picture of various planes of analysis are given. Plane-1 and plane-2 are the vertical planes along the two corridors. Plane-3 and plane-4 are the horizontal planes at the middle level of the height of the top and bottom floor respectively.

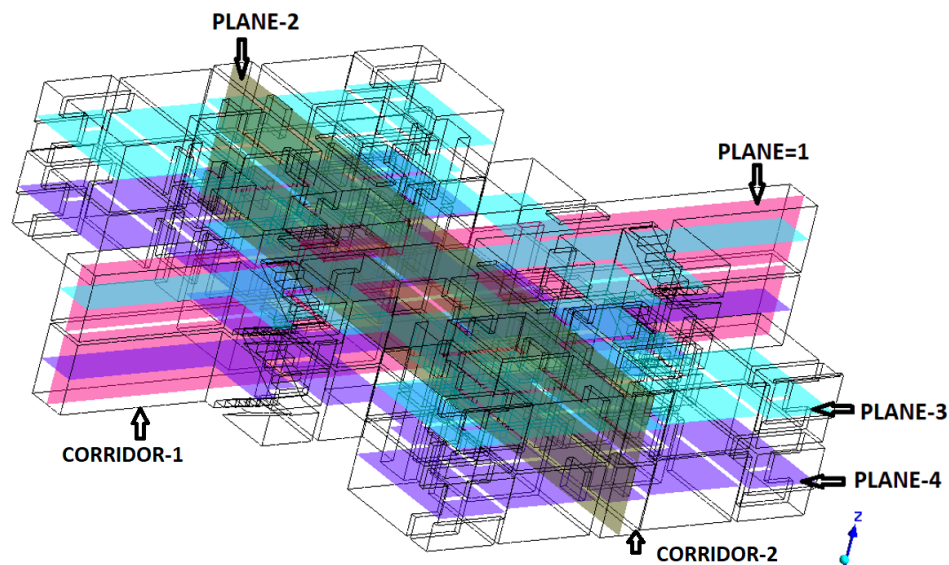


Fig. 5. Various planes for analysis

Figure 6 (a-c) shows the velocity, pressure and temperature distribution on plane-1 for case-A-2. It can be observed that the air is pulled through the inlet of the corridor towards the centre on both floors as shown in Figure 6(a). On the bottom floor, it can be visualized that the airflow occurs from both sides of the corridor-1 and the air flows also from both sides of another corridor that is placed perpendicularly. Therefore, the air reverts from the centre due to the reasons

- i. obstacle imposed by the airflow of corridor-2
- ii. impact between two opposite airflow streams in corridor-1.

The reverted air moves in the upward direction through the corridor vents present in front of the doors/windows. On the top floor, the corridor air movement along the horizontal direction is restricted by the upward airflow. Hence the two recirculation zones are observed just left and right of the mid position on the top floor.

The pressure contour shown in Figure 6(b) reveals that where the pressure is high, at that region, the velocity becomes less and it happens because the flow always follows Bernoulli's principle. However, the high-pressure and the low-velocity region are mainly observed closer to the roof. From Figure 6(c) it is observed that the temperature of the air closer to the roof is high but not high near the floor region though the entire wall region has the same temperature. The air closer to the wall gained heat and its temperature rises. Hence the density of air closer to the wall region decreases and becomes lighter. The hot light air always floats over the heavier cold air. Therefore, the air neither comes down due to its lightweight nor moves up due to the flow restriction provided by the roof. As a result, the pressure becomes high closer to the bottom portion of the roof. On the other hand, the hot light air closer to the floor area moves up and also moves in the horizontal direction to follow the flow path. So, the new fresh air enters continuously into the corridor and keeps the floor region cool as shown in Figure 6(c). Due to the flow velocity difference between the upper layer and lower layer air, a low-pressure recirculation zone is observed under the roof near the inlet region of both floors. Therefore, a fraction of air moves out from the corridor to the ambiance under the roof.

The high-pressure region below the roof of the top floor is relatively larger than the bottom floor. Because, the airflow stream from the bottom to the top floor through the vent, restricts the horizontal airflow at the top floor.

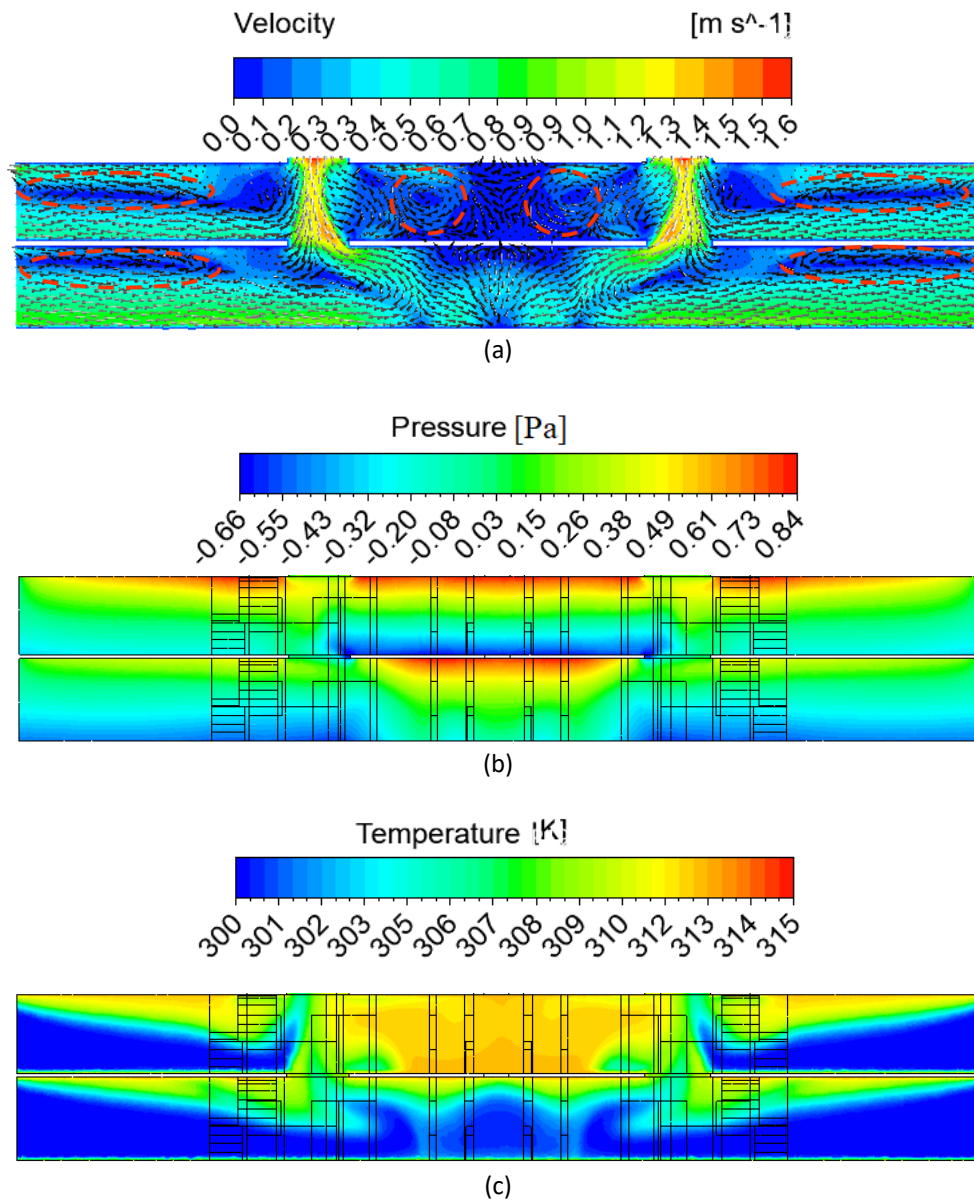


Fig. 6. (a) velocity distribution, (b) pressure distribution (c) temperature distribution on plane-1 for the case of corridor roof opening in front of doors, windows and balcony only with $\Delta T=15^{\circ}\text{C}$

A similar kind of airflow pattern, pressure distribution and temperature field like plane-1 is also observed in another plane (Plane-2) as shown in Figure 7(a). Here also it can be observed that the velocity and pressure relation exist following Bernoulli's principle. The recirculation zones are also observed under the roofs where the temperature is high.

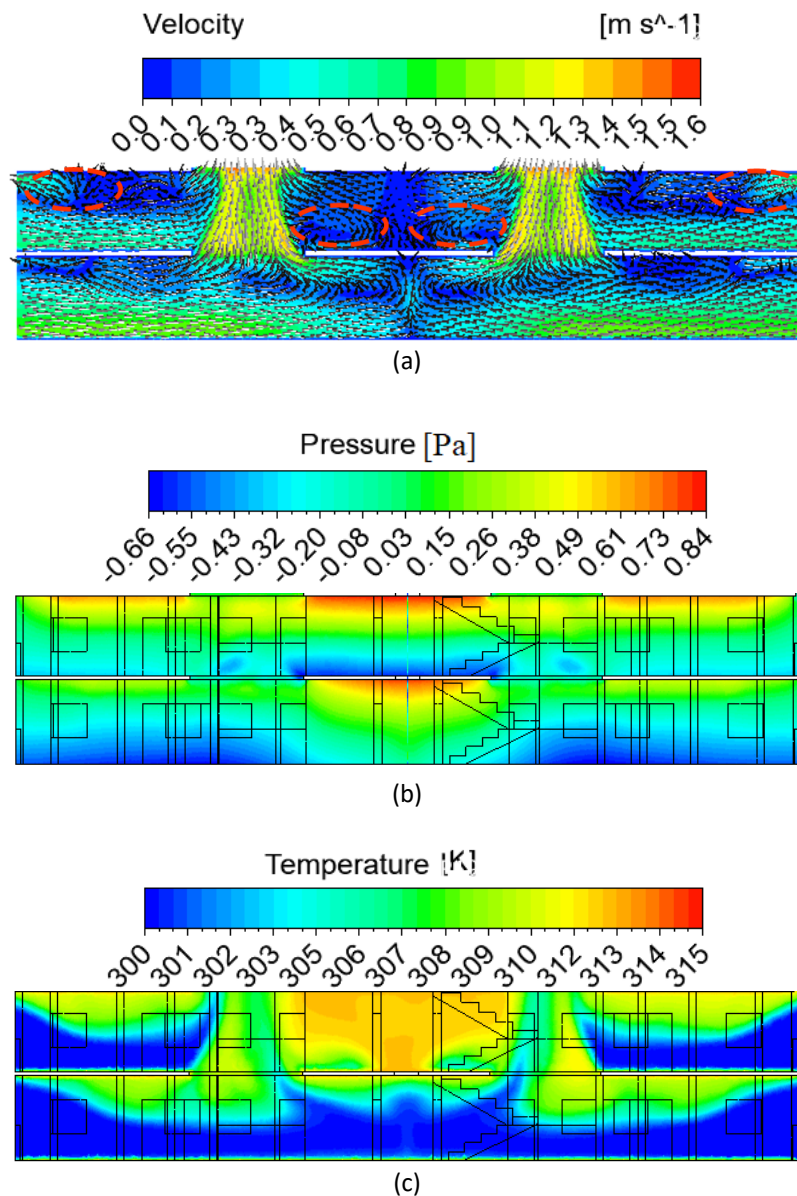


Fig. 7. (a) velocity distribution, (b) pressure distribution (c) temperature distribution on plane-2 for the case of corridor roof opening in front of doors, windows and balcony only with $\Delta T=15^{\circ}\text{C}$

Figure 8(a and b) shows the velocity distribution on plane-4 (mid-plane on the bottom floor) and plane-3 (mid-plane on the top floor) respectively for case-A-2. It has been observed that the flow pattern is symmetric about the corridors as all four flats have the same floor plan. It is observed that the airflow towards the centre of both corridors is smooth at the bottom floor analysis plane (Plane-4). The high-velocity region (red patch) at plane-3 (upper floor analysis plane) as shown in Figure 8(b) is nothing but the upward air movement through the vents. This upward movement is also shown in Figures 6(a) and 7(a). Therefore, due to the flow restriction offered by the upward flow air stream, the airflow through both corridors could not reach the centre point. As a result, the airflow distribution becomes poor on the top floor as compared to the bottom floor. Mainly the flow restriction affects the ventilation of the living room as compared to other rooms. However, the bed room-1 seems to be the least ventilated place on both of the floors as it is far away from the corridor. The maximum flow velocity is around 0.5 m/s inside the rooms. The areas inside the rooms, closer to the corridor are well-ventilated.

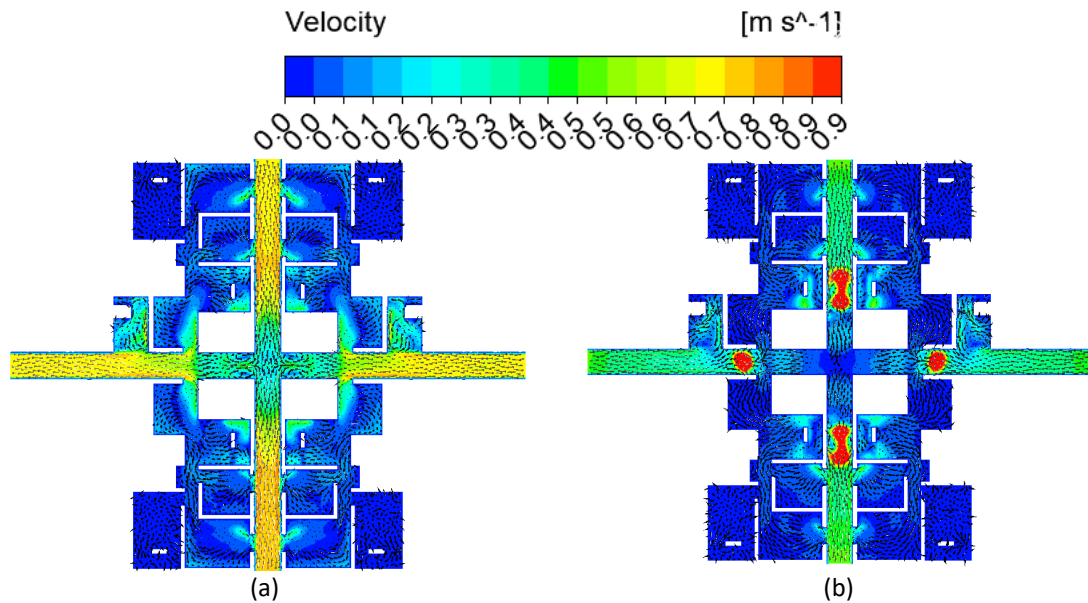
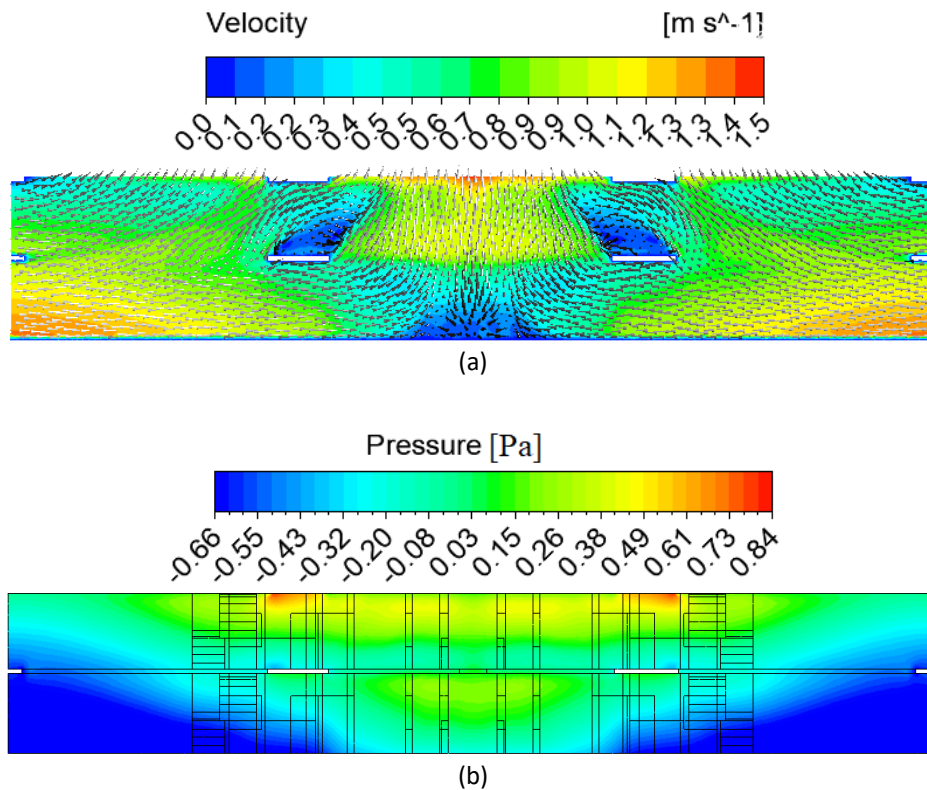


Fig. 8. (a) velocity distribution, (b) pressure distribution (c) temperature distribution on (a) plane-4 (b) plane-3 for the case of corridor roof opening in front of doors, windows and balcony only with $\Delta T=15^{\circ}\text{C}$

Figure 9(a-c) and Figure 10(a-c) show the velocity field, pressure field and temperature distribution across the two perpendicular planes; plane-1 and plane-2 respectively for case-B-2. In case-B-2, the corridor vents are provided in the remaining areas except for the areas in front of the doors and windows. Therefore, in comparison with case-A-2, wide vent opening provisions are there in case-B. Plane-1 and plane-2 are the planes along two corridors.



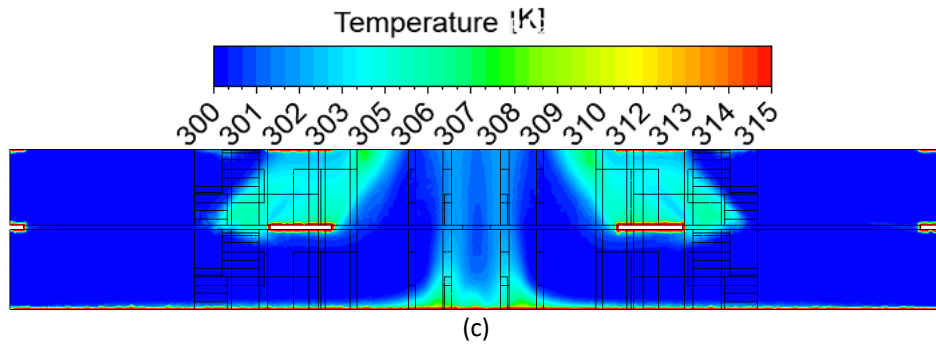
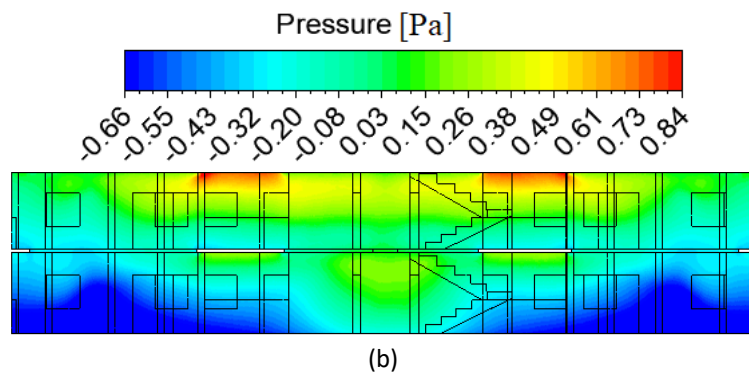
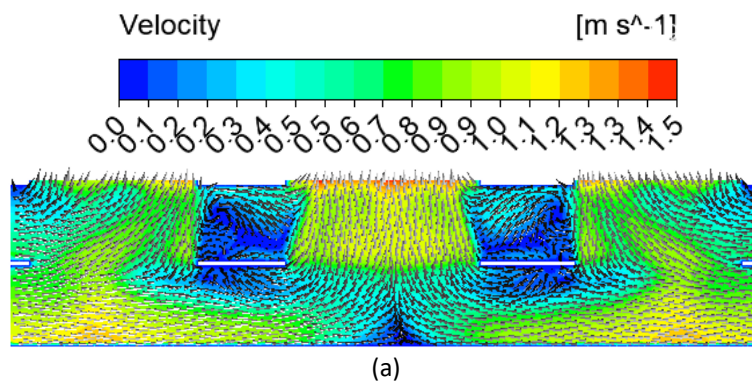


Fig. 9. (a) velocity distribution, (b) pressure distribution (c) temperature distribution on plane-1 for the case of corridor roof opening except in front of doors, windows and balcony only with $\Delta T=15^\circ\text{C}$

From Figures 9 and 10, it has been observed that in the region where pressure is high, velocity becomes less and vice versa. A high-pressure zone is observed below the roof on both floors. Because the hot light air cannot come down due to its lightweight and cannot move up due to the roof restriction. As a result, a high-pressure stagnation zone occurs below the roof. As compared to case-A, in case of B, a small high-pressure region is observed due to less roof area.



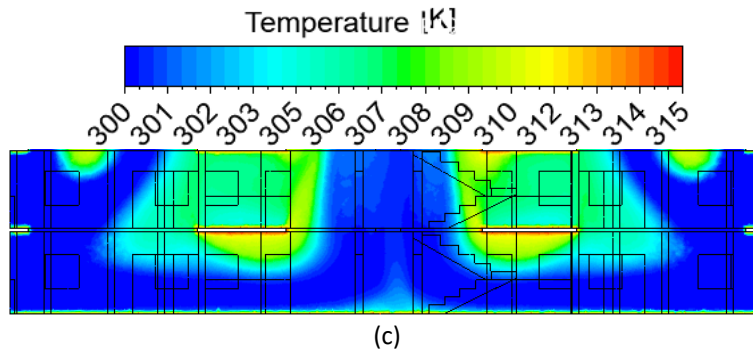


Fig. 10. (a) velocity distribution, (b) pressure distribution (c) temperature distribution on plane-2 for the case of corridor roof opening except in front of doors, windows and balcony only with $\Delta T=15^\circ\text{C}$

Figures 11(a and b) show the velocity distribution on plane-4 (mid-plane on the bottom floor) and plane-3 (mid-plane on the top floor) respectively for case-B-2. The flow pattern is observed as symmetric about the corridors. It is observed that through the ground floor corridor, the airflows smoothly towards the centre and the flow velocity continuously decreases. Because part of the air moves upward direction through the vent due to buoyancy and part of the air enters the rooms as well. On the other hand, in plane-3 (top floor plane), the corridor air could not reach the centre because the entire air enters through the top floor corridor and moves out through the vent vertically. However, a high-velocity region is observed near the centre and this is the air moving upward direction from the bottom floor. It is observed that the bottom floor houses are well-ventilated as compared to the top floor near the corridor. Here, the maximum air velocity inside the rooms is around 0.5 m/s.

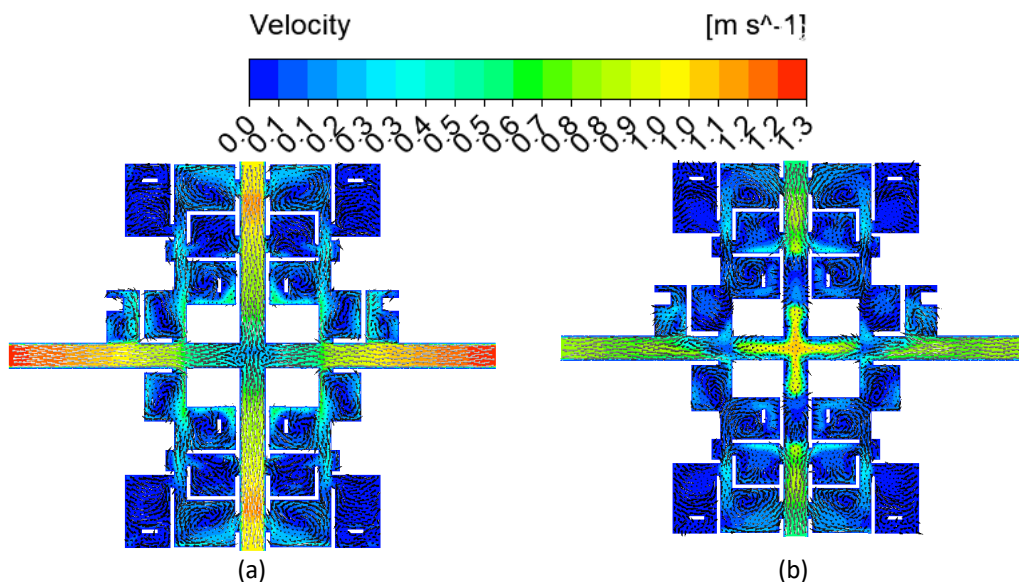


Fig. 11. Velocity vector and contour on (a) plane-4 (b) plane-3 for the case of corridor roof opening except in front of doors, windows and balcony only with $\Delta T=15^\circ\text{C}$

Figure 12 and 13 shows the velocity variation along the midline of corridor-1 and corridor-2 respectively for the different temperature difference between the wall and inside air (various ΔT for cases A-1, A-2 and A-3). These are the cases of vent opening in front of the door/windows only. Two peak velocity regions are observed in both figures.

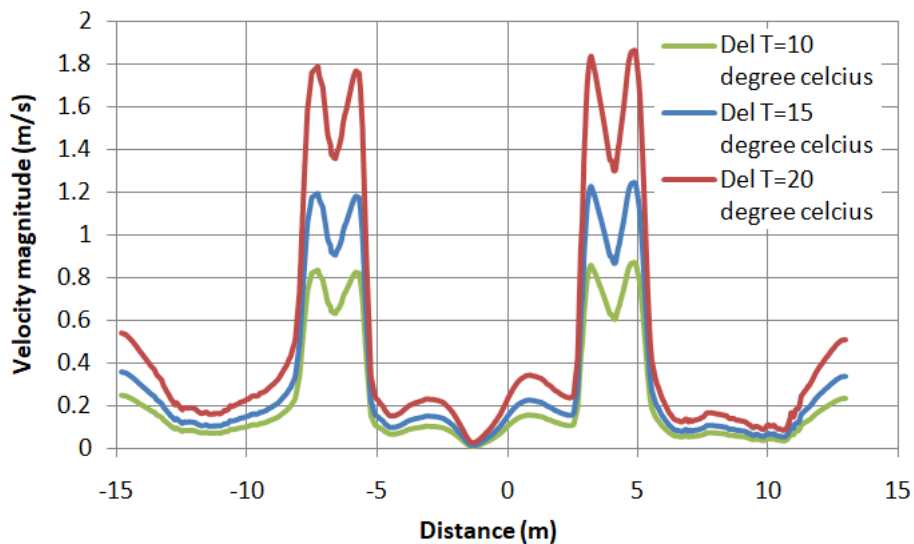


Fig. 12. Velocity plane-1 for the case of corridor roof opening in front of doors, windows and balcony at $\Delta T=10^{\circ}\text{C}$, $\Delta T=15^{\circ}\text{C}$, $\Delta T=20^{\circ}\text{C}$

These are the region at the corridor vent position. It is also observed that with increase in ΔT , the velocity difference increases throughout the length. Velocity at the vent region increases around 55% when the ΔT difference increases 10°C . When the ΔT difference is 5°C , the velocity increment is observed as 33%. However, the increment in velocity other than the vent region is less than 10% with increase in ΔT .

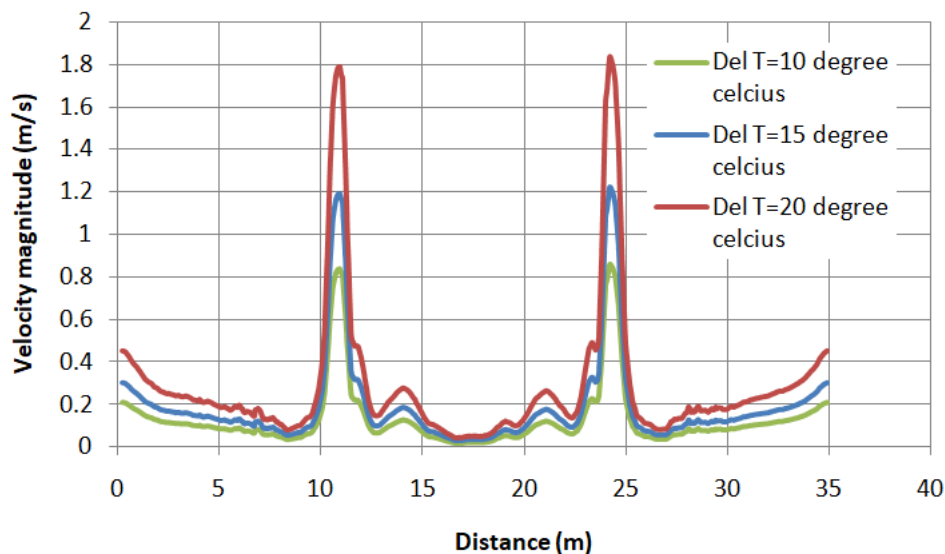


Fig. 13. Velocity plane-2 for the case of corridor roof opening in front of doors, windows and balcony at $\Delta T=10^{\circ}\text{C}$, $\Delta T=15^{\circ}\text{C}$, $\Delta T=20^{\circ}\text{C}$

Figure 14 and 15 shows the velocity variation along the midline of corridor-1 and corridor-2 respectively for the different temperature difference between the wall and inside air (various ΔT for cases A-1, A-2 and A-3). Cases A-1 to A-3 are the cases of corridor vent opening in the areas except for the area in front of doors and windows. Here, the high velocity at three large vent openings is observed.

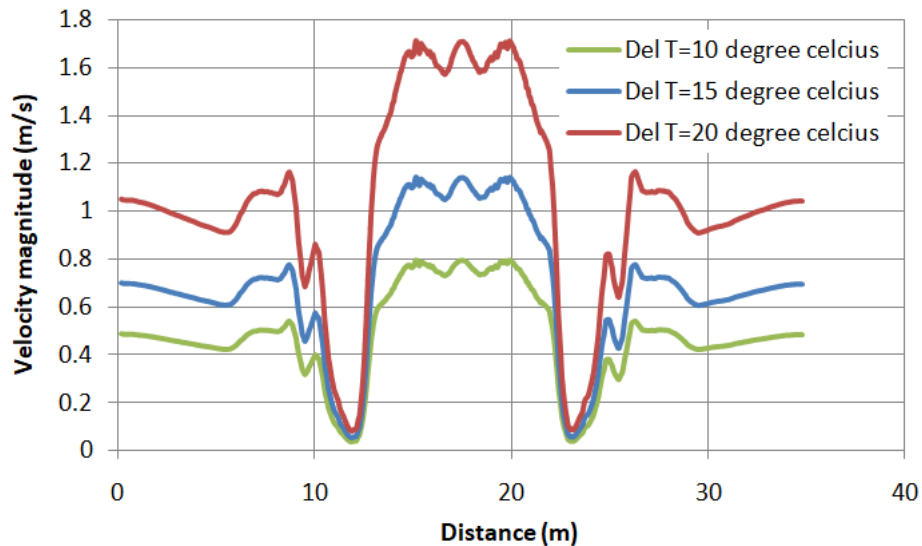


Fig. 14. Velocity plane-2 for the case of corridor roof opening except in front of doors, windows and balcony at $\Delta T=10^{\circ}\text{C}$, $\Delta T=15^{\circ}\text{C}$, $\Delta T=20^{\circ}\text{C}$

It is observed that through the central vent, the velocity is very high. Here also it is observed that with increase in ΔT , the velocity increases. The velocity increases around 50% at the central vent region, when ΔT variation is 10°C . Near side vents this variation is around 30% maximum.

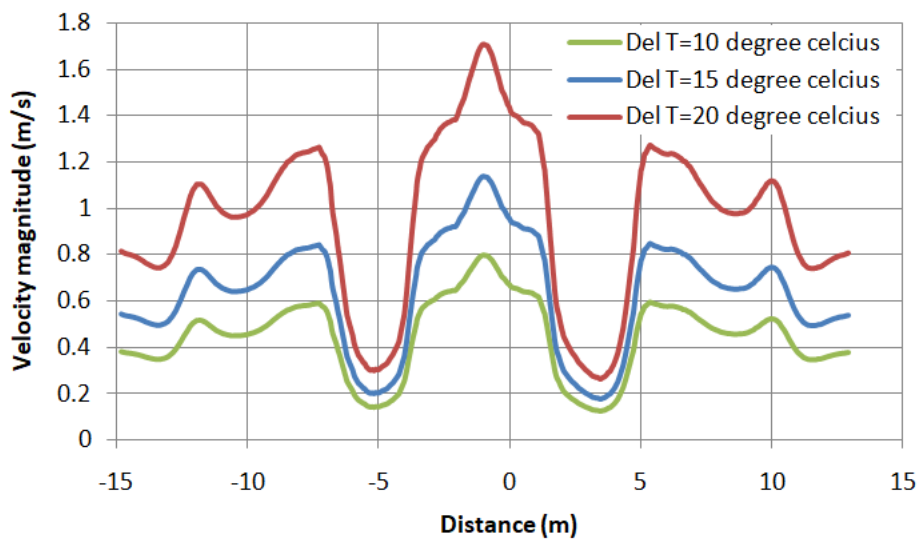


Fig. 15. Velocity plane-1 for the case of corridor roof opening except in front of doors, windows and balcony at $\Delta T=10^{\circ}\text{C}$, $\Delta T=15^{\circ}\text{C}$, $\Delta T=20^{\circ}\text{C}$

Figure 16 shows three different air velocity regions (<0.2 m/s, $0.2-1$ m/s and >1 m/s) in plane-3 and plane-4 for different ΔT for the case of corridor vent opening in the area except in the area in front of the doors and windows (Case-B-1 to B-3).

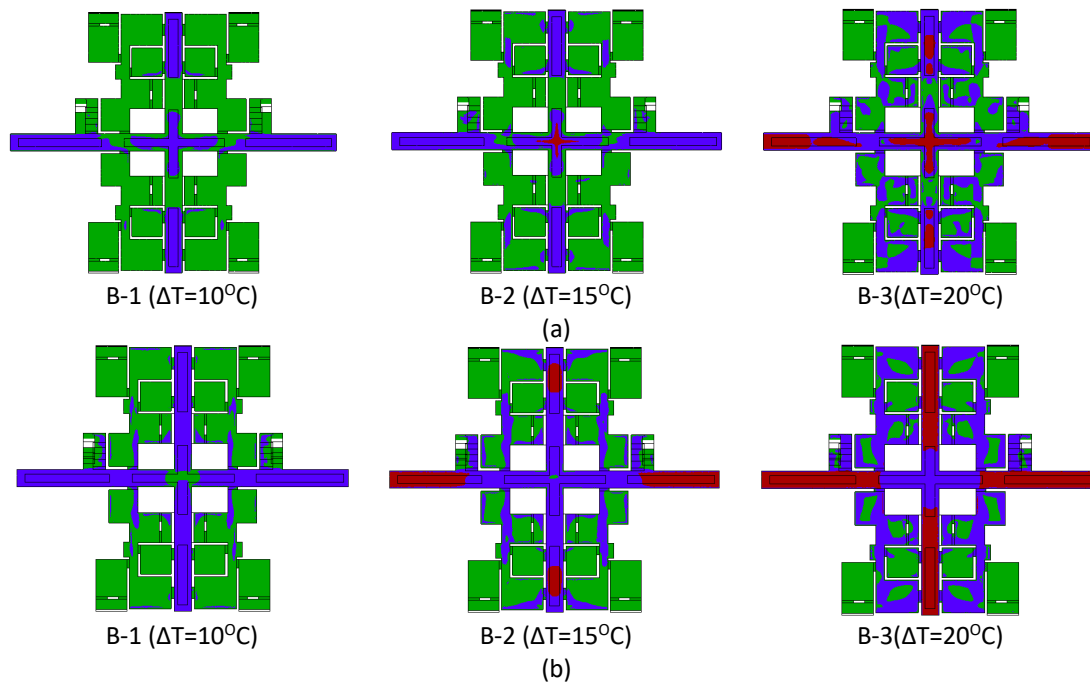


Fig. 16. Area covered with different airflow velocity (Green $< 0.2 \text{ m/s}$, Blue $0.2-1 \text{ m/s}$, Brown $> 1 \text{ m/s}$) at (a) Plane-3 and (b) Plane-4 for $\Delta T=10^\circ\text{C}$, $\Delta T=15^\circ\text{C}$, $\Delta T=20^\circ\text{C}$

Figure 17 shows different airflow velocity-covered areas in percentage at plane-3 and plane-4 for different ΔT conditions. It is observed that with $\Delta T=10^\circ\text{C}$, no area is covered with a flow velocity greater than 1 m/s either on plane-1 and plane-2 either plane-3 or plane-4. In Figure 17 it is also been seen that 0% area covered with flow velocity greater than 1 m/s in both planes. With $\Delta T=10^\circ\text{C}$, around 80% and 76% area are covered with ultra-low velocity region ($< 1 \text{ m/s}$) in plane-3 and plane-4 respectively. It is observed that the ultra-low velocity area decreases and the velocity area covered with $0.2-1.0 \text{ m/s}$ and $> 1 \text{ m/s}$ increases with increase in ΔT . With $\Delta T=20^\circ\text{C}$, around 16% and 20% area are covered with high velocity on plane-3 and plane-4 respectively. However, the low velocity ($< 0.1 \text{ m/s}$) on plane-3 is higher as compared to plane-4 irrespective of ΔT . On the other hand, the velocity region $0.2-1 \text{ m/s}$ and greater than 1 m/s is higher in plane-3 than plane-4 with increase in ΔT .

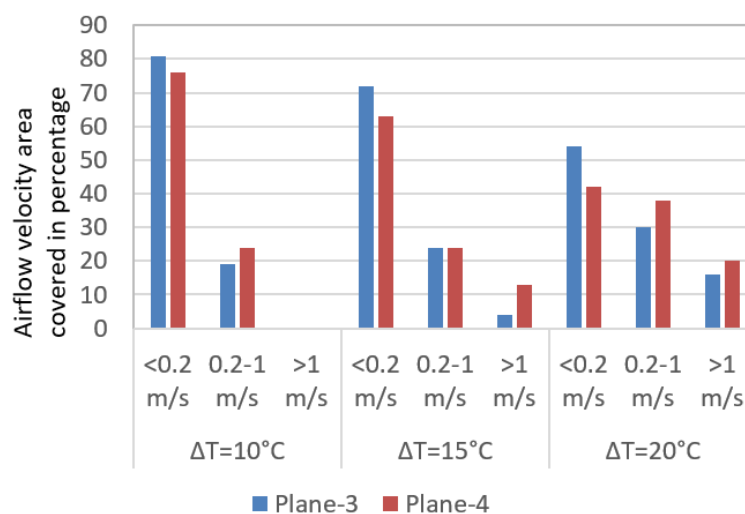


Fig. 17. Airflow velocity ($< 0.2 \text{ m/s}$, $0.2-1 \text{ m/s}$, $> 1 \text{ m/s}$) area covered in percentage at plane-3 and plane-4 for $\Delta T=10^\circ\text{C}$, $\Delta T=15^\circ\text{C}$, $\Delta T=20^\circ\text{C}$

Air charge per hour (ACH) into the corridor is evaluated in CFM (cubic feet per minute with different such as; $\Delta T=10^{\circ}\text{C}$, $\Delta T=15^{\circ}\text{C}$, $\Delta T=20^{\circ}\text{C}$ for both case-A and Case-B as shown in Figure 18. It is evaluated as;

$$CH = \frac{(\dot{m}/\rho) \times 3600}{\text{Total Volume of the airflow space in ft cube}} \quad (8)$$

Where, \dot{m} is the total mass flow rate through outlet vents in kg/s., ρ is the average density of the air in kg/ft³. The total volume of the computational domain is evaluated as 82776.519 cubic feet and the total mass flow rate from the vent outlet is evaluated as 14.905 kg/s.

From the figure, it has been observed that for case-B (Large corridor vent opening), the ACH is always on the higher side than case-A. In all ΔT conditions, the ACH is higher than the standard ACH (ACH>2). When the temperature difference rises from $\Delta T=10^{\circ}\text{C}$ to $\Delta T=20^{\circ}\text{C}$, the ACH rises 53.45% for case-A. For case-B, it rises to 45.52%.

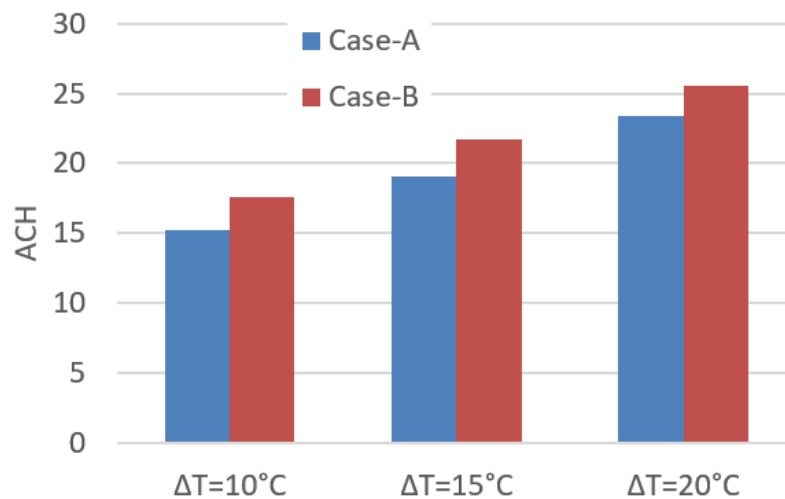


Fig. 18. ACH of the whole building including corridor with different ΔT condition for case-A and case-B

6. Conclusion

Computational simulations have been performed for an apartment building to study the stack ventilation through corridor vent opening caused by the temperature difference between wall and room air temperature. Two types of corridor openings are used

- i. corridor opening in front of the doors/windows of the house
- ii. corridor opening in the remaining areas except for the area in front of the doors/windows.

Three different temperature differences between the wall and inside air such as; $\Delta T=10^{\circ}\text{C}$, $\Delta T=15^{\circ}\text{C}$, $\Delta T=20^{\circ}\text{C}$ are used.

From the investigation it has been observed that;

- i. At the bottom floor, the air entering through the corridor can move towards the centre whereas, at the upper floor, it cannot reach the central position because the flow is restricted by an upward air stream through the corridor vent.

- ii. For Case-A (corridor opening in front of the doors/windows of the house), the recirculation zones are observed below the roof of the upper floor. The light hot air closer to the roof neither moves up due to the restriction of the floor nor comes down because it is lighter. Hence, recirculation occurs and due to this, a part of the air moves out through the inlet closer to the roof. On the other hand, for Case-B, due to the large vent opening, these recirculation zones are not observed.
- iii. As ΔT increases, irrespective of corridor vent position, the airflow rate becomes better at the corridor as well as in the rooms. 0% area covered with flow velocity greater than 1 m/s in both bottom and upper floor planes. With $\Delta T=10^\circ\text{C}$, around 80% and 76% area is covered with ultra-low velocity region (< 1 m/s) in plane-3 (upper floor plane) and plane-4 (lower floor plane) respectively. With $\Delta T=20^\circ\text{C}$, around 16% and 20% area are covered with high velocity on plane-3 and plane-4 respectively.
- iv. ACH increases, as the corridor vent opening area increases. When the temperature difference rises from $\Delta T=10^\circ\text{C}$ to $\Delta T=20^\circ\text{C}$, the ACH rises 53.45% for case-A. For case-B, it rises to 45.52%.

Acknowledgement

This research was not funded by any grant.

References

- [1] Li, Jing, Jia-ping Liu, and Yu Liu. "Research on building heating energy option of lhaza and development energy management tools." In *2009 International Conference on Management and Service Science*, pp. 1-4. IEEE, 2009. <https://doi.org/10.1109/ICMSS.2009.5305162>
- [2] Franco, Sainu, Venkata Ravibabu Mandla, and K. Ram Mohan Rao. "Urbanization, energy consumption and emissions in the Indian context A review." *Renewable and Sustainable Energy Reviews* 71 (2017): 898-907. <https://doi.org/10.1016/j.rser.2016.12.117>
- [3] Pode, Ramchandra. "Addressing India's energy security and options for decreasing energy dependency." *Renewable and Sustainable Energy Reviews* 14, no. 9 (2010): 3014-3022. <https://doi.org/10.1016/j.rser.2010.07.007>
- [4] Ghazali, Azhar, Wan Muhd Zakwan Wan Zin, and Mazran Ismail. "Indoor Thermal Comfort Perception at Atrium Zone: Case Study of Naturally Ventilated Public Market." *Journal of Advanced Research in Applied Sciences and Engineering Technology* 29, no. 1 (2022): 13-29. <https://doi.org/10.37934/araset.29.1.1329>
- [5] Walker, Christine, Gang Tan, and Leon Glicksman. "Reduced-scale building model and numerical investigations to buoyancy-driven natural ventilation." *Energy and Buildings* 43, no. 9 (2011): 2404-2413. <https://doi.org/10.1016/j.enbuild.2011.05.022>
- [6] Liu, Pei-Chun, Hsien-Te Lin, and Jung-Hua Chou. "Evaluation of buoyancy-driven ventilation in atrium buildings using computational fluid dynamics and reduced-scale air model." *Building and Environment* 44, no. 9 (2009): 1970-1979. <https://doi.org/10.1016/j.buildenv.2009.01.013>
- [7] Acred, Andrew, and Gary R. Hunt. "A simplified mathematical approach for modelling stack ventilation in multi-compartment buildings." *Building and Environment* 71 (2014): 121-130. <https://doi.org/10.1016/j.buildenv.2013.09.004>
- [8] Yang, Dong, and Ping Li. "Natural ventilation of lower-level floors assisted by the mechanical ventilation of upper-level floors via a stack." *Energy and buildings* 92 (2015): 296-305. <https://doi.org/10.1016/j.enbuild.2015.01.065>
- [9] Tovar, T., and CA Campo Garrido. "Stack-driven ventilation in two interconnected rooms sharing a single opening and connected to the exterior by a lower vent." *International Journal of Ventilation* 9, no. 3 (2010): 211-226. <https://doi.org/10.1080/14733315.2010.11683881>
- [10] Pu, Jing, Yanping Yuan, Fujian Jiang, Kaijie Zheng, and Kaiming Zhao. "Buoyancy-driven natural ventilation characteristics of thermal corridors in industrial buildings." *Journal of Building Engineering* 50 (2022): 104107. <https://doi.org/10.1016/j.jobe.2022.104107>
- [11] Kotani, Hisashi, Ryuji Satoh, and Toshio Yamanaka. "Natural ventilation of light well in high-rise apartment building." *Energy and Buildings* 35, no. 4 (2003): 427-434. [https://doi.org/10.1016/S0378-7788\(02\)00166-4](https://doi.org/10.1016/S0378-7788(02)00166-4)

- [12] Fitzgerald, Shaun D., and Andrew W. Woods. "The influence of stacks on flow patterns and stratification associated with natural ventilation." *Building and Environment* 43, no. 10 (2008): 1719-1733. <https://doi.org/10.1016/j.buildenv.2007.10.021>
- [13] Schulze, Tobias, and Ursula Eicker. "Controlled natural ventilation for energy efficient buildings." *Energy and buildings* 56 (2013): 221-232. <https://doi.org/10.1016/j.enbuild.2012.07.044>
- [14] Bayoumi, Mohannad. "Improving indoor air quality in classrooms via wind-induced natural ventilation." *Modelling and Simulation in Engineering* 2021 (2021): 1-14. <https://doi.org/10.1155/2021/6668031>
- [15] Nashee, Sarah Rabee, and Haiyder Minin Hmood. "Numerical Study of Heat Transfer and Fluid Flow over Circular Cylinders in 2D Cross Flow." *Journal of Advanced Research in Applied Sciences and Engineering Technology* 30, no. 2 (2023): 216-224. <https://doi.org/10.37934/araset.30.2.216224>
- [16] Shabri, Muhamad Silmie Mohamad, Mohd Al Hafiz Mohd Naw, Mohd Shahir Kasim, Khor Chu Yee, Mohd Uzair Mohd Rosli, Mohammad Azrul Rizal Alias, and Raja Muhammad Zulkifli Raja Ibrahim. "Multi-Stage Swirling Fluidized Bed: Part 1-Numerical Analysis Procedure." *Journal of Advanced Research in Applied Sciences and Engineering Technology* 30, no. 1 (2023): 65-75. <https://doi.org/10.37934/araset.30.1.6575>
- [17] Ahmed, Alaaeldeen Mohamed Elhadad. "Resistance Evaluation for the Submerged Glider System using CFD Modelling." *Journal of Advanced Research in Applied Sciences and Engineering Technology* 29, no. 3 (2023): 147-159. <https://doi.org/10.37934/araset.29.3.147159>
- [18] Kadir, Muhammad Rashidi Abdul, Mugabe Jean Paul, Mohamad Ikhwan Kori, Kahar Osman, Aizai Azan Abdul Rahim, and Ahmad Zahran Md Khudzari. "Numerical Study on the Effect of Miniaturized Impeller Diameter on Mechanical Performance in a Left Ventricular Assist Device." *Journal of Advanced Research in Applied Sciences and Engineering Technology* 28, no. 2 (2022): 26-33. <https://doi.org/10.37934/araset.28.2.2633>
- [19] Bayoumi, Mohannad. "Improving Natural Ventilation Conditions on Semi-Outdoor and Indoor Levels in Warm-Humid Climates." *Buildings* 8, no. 6 (2018): 75. <https://doi.org/10.3390/buildings8060075>
- [20] Hussain, Shafqat, and Patrick H. Oosthuizen. "Validation of numerical modeling of conditions in an atrium space with a hybrid ventilation system." *Building and Environment* 52 (2012): 152-161. <https://doi.org/10.1016/j.buildenv.2011.12.016>
- [21] Acred, Andrew, and Gary R. Hunt. "Multiple flow regimes in stack ventilation of multi-storey atrium buildings." *International Journal of Ventilation* 12, no. 1 (2013): 31-40. <https://doi.org/10.1080/14733315.2013.11684000>
- [22] Wawrzyniak, Zbigniew M., Grzegorz Borowik, Eliza Szczechla, Paweł Michalak, Radosław Pytlak, Paweł Cichosz, Dobiesław Ircha, Wojciech Olszewski, and Emilian Perkowski. "Relationships between crime and everyday factors." In *2018 IEEE 22nd International Conference on Intelligent Engineering Systems (INES)*, pp. 000039-000044. IEEE, 2018. <https://doi.org/10.1109/INES.2018.8523999>
- [23] Toftum, Jorn, and P. Ole Fanger. "Air humidity requirements for human comfort." *ASHRAE transactions* 105 (1999): 641.
- [24] Ghose, Prakash, Jitendra Patra, Amitava Datta, and Achintya Mukhopadhyay. "Effect of air flow distribution on soot formation and radiative heat transfer in a model liquid fuel spray combustor firing kerosene." *International Journal of Heat and Mass Transfer* 74 (2014): 143-155. <https://doi.org/10.1016/j.ijheatmasstransfer.2014.03.001>
- [25] Soleimani, Zohreh, John Kaiser Calautit, and Ben Richard Hughes. "Computational analysis of natural ventilation flows in geodesic dome building in hot climates." *Computation* 4, no. 3 (2016): 31. <https://doi.org/10.3390/computation4030031>
- [26] Yang, Tong, Nigel G. Wright, David W. Etheridge, and Andrew D. Quinn. "A comparison of CFD and full-scale measurements for analysis of natural ventilation." *International Journal of Ventilation* 4, no. 4 (2006): 337-348. <https://doi.org/10.1080/14733315.2005.11683713>
- [27] Horan, Joseph M., and Donal P. Finn. "CFD reliability issues in the prediction of airflows in a naturally ventilated building." *International Journal of Ventilation* 4, no. 3 (2005): 255-268. <https://doi.org/10.1080/14733315.2005.12021996>